Sterol and pH Interdependence in the Binding, Oligomerization, and Pore Formation of Listeriolysin O[†]

Andrej Bavdek,[‡] Nelson O. Gekara,[§] Dragan Priselac,[‡] Ion Gutiérrez Aguirre,[‡,||] Ayub Darji,[⊥] Trinad Chakraborty,[⊥] Peter Maček,[‡] Jeremy H. Lakey,[@] Siegfried Weiss,[§] and Gregor Anderluh*,[‡]

Department of Biology, Biotechnical Faculty, University of Ljubljana, Večna pot 111, 1000 Ljubljana, Slovenia, Helmholtz Centre for Infectious Research, Mascheroder Weg 1, D-38124 Braunschweig, Germany, Institute for Medical Microbiology, University Giessen, Frankfurterstrasse 107, D-35392 Giessen, Germany, and Institute for Cell and Molecular Biosciences, University of Newcastle upon Tyne, Framlington Place, Newcastle upon Tyne NE2 4HH, U.K.

ABSTRACT: Listeriolysin O (LLO) is the most important virulence factor of the intracellular pathogen *Listeria monocytogenes*. Its main task is to enable escape of bacteria from the phagosomal vacuole into the cytoplasm. LLO belongs to the cholesterol-dependent cytolysin (CDC) family but differs from other members, as it exhibits optimal activity at low pH. Its pore forming ability at higher pH values has been largely disregarded in *Listeria* pathogenesis. Here we show that high cholesterol concentrations in the membrane restore the low activity of LLO at high pH values. LLO binds to lipid membranes, at physiological or even slightly basic pH values, in a cholesterol-dependent fashion. Binding, insertion into lipid monolayers, and permeabilization of calcein-loaded liposomes are maximal above approximately 35 mol % cholesterol, a concentration range typically found in lipid rafts. The narrow transition region of cholesterol concentration separating low and high activity indicates that cholesterol not only allows the binding of LLO to membranes but also affects other steps in pore formation. We were able to detect some of these by surface plasmon resonance-based assays. In particular, we show that LLO recognition of cholesterol is determined by the most exposed 3β-hydroxy group of cholesterol. In addition, LLO binds and permeabilizes J774 cells and human erythrocytes in a cholesterol-dependent fashion at physiological or slightly basic pH values. The results clearly show that LLO activity at physiological pH cannot be neglected and that its action at sites distal to cell entry may have important physiological consequences for *Listeria* pathogenesis.

Listeria monocytogenes is the causative agent of the food-borne disease listeriosis. It is a facultative intracellular pathogen with a complex life cycle. Several virulence factors promote distinct steps in its parasitism (*1*). After the entry into the cell by phagocytosis, it needs to escape from the vacuole into the cytosol for efficient growth and spread to other cells. This is achieved by secretion of the pore-forming toxin (PFT)[1] listeriolysin O (LLO), which destroys the phagosomal membrane and is thus the most critical factor for the escape from phagocytic vacuoles (*2−6*).

LLO belongs to a family of cholesterol-dependent cytolysins (CDC) secreted by Gram-positive bacteria (*7*, *8*). More than 20 members have been described, including perfringolysin from *Clostridium perfringens*, streptolysin O from *Streptococcus pyogenes*, pneumolysin from *Streptococcus pneumoniae*, etc. The common features of the CDC protein family are cholesterol dependence of cytolytic activity, hence the name CDC, and a conserved undecapeptide motif at the tip of the molecule that was implicated in cell membrane binding (*9*, *10*). CDC are synthesized as monomers but are able to undergo a structural transformation on the surface of the target cells, ultimately leading to aggregation and formation of transmembrane pores that cause toxicity (*11*, *12*). They are all large proteins with molecular masses of >50 kDa. The available three-dimensional structures of perfringolysin and intermedilysin from *Streptococcus intermedius* revealed an elongated β-sheet-rich molecule organized in four domains (*9*, *13*). Domain 4 promotes initial binding to the cholesterol-containing membranes (*14−16*). After the binding, monomers diffuse in the plane of the

* To whom correspondence should be addressed: Department of Biology, Biotechnical Faculty, University of Ljubljana, Večna pot 111, 1000 Ljubljana, Slovenia. Telephone: 00386 1 423 33 88. Fax: 00386 1 257 33 90. E-mail: gregor.anderluh@bf.uni-lj.si.

[‡] University of Ljubljana.
[§] Helmholtz Centre for Infectious Research.
[||] Present address: Department of of Plant Physiology and Biotechnology, National Institute of Biology, Večna pot 111, 1000 Ljubljana, Slovenia.
[⊥] University Giessen.
[@] University of Newcastle upon Tyne.

[1] Abbreviations: BSA, bovine serum albumin; CDC, cholesterol-dependent cytolysins; DOPC, 1,2-dioleoyl-*sn*-glycero-3-phosphocholine; DTT, dithiothreitol; HA, hemagglutinin; LLO, listeriolysin O; LUV, large unilamellar vesicles; PFT, pore-forming toxin; POPC, 1,2-palmitoyl-*sn*-glycero-3-phosphocholine; RU, resonance unit; SPR, surface plasmon resonance; streptavidin-PE, streptavidin-phycoerythrin.

membrane to form a prepore complex (*17*), and finally, each monomer contributes two β-hairpins, formed from two pairs of α-helices from domain 3, to form a final oligomeric β-barrel pore (*18*, *19*). Pores formed by CDC are large structures with a diameter of 25−35 nm and are composed of 35−50 monomers (*7*, *8*). LLO has an acidic pH optimum of activity (*5*, *20−22*), and this unique property in the CDC family (*7*) ensures maximal activity in phagocytic vacuoles and low activity in the cytoplasm of the host cells. LLO in addition possesses a proline-glutamate-serine-threonine (PEST) sequence that is thought to promote its degradation in the cytoplasm (*23*). Both features ensure that the host cell is not affected by free LLO once the phagocytic vacuole is destroyed.

Although the main task of LLO is to enable the escape of bacteria from phagosomes, evidence accumulated in recent years suggests that it also has other roles in *Listeria* pathogenesis. LLO was found to bind to cholesterol-rich caveolae (*24*) and to lipid rafts (*25*, *26*). LLO also aggregated rafts and triggered cell signaling (*26*). It was also shown that at low concentrations LLO forms pores in the plasma membrane of various cells (*27*, *28*). These pores were permeable to Ca^{2+}, and this may explain the wide variety of Ca^{2+}-dependent cellular responses observed after exposure to LLO, i.e., effects on bacterial internalization (*29*, *30*), induction of mucin exocytosis in epithelial intestinal cells (*24*), induction of cytokine gene expression in macrophages (*31*, *32*), induction of apoptosis (*33*, *34*), etc. During infection, the pore forming activity of LLO is not restricted to the phagosome. LLO can be secreted into serum by extracellular bacteria or dead infected cells, thus interacting with bystander cells at distal sites. LLO pore forming activity at distal sites and suboptimal pH may, therefore, be important for host−parasite interactions.

In this paper, we explore LLO binding and pore formation at suboptimal pH and various cholesterol concentrations *in vitro*. At physiological and slightly basic pH values, LLO still readily binds to natural and model lipid membranes in a cholesterol-dependent fashion and forms calcein permeable pores. A distinct threshold concentration of cholesterol is needed for efficient binding, insertion, and pore formation. Results showed that LLO is able to efficiently form pores at alkaline pH in membranes with the high concentrations of cholesterol found typically in plasma membrane lipid rafts.

MATERIALS AND METHODS

Materials.   1,2-Dioleoyl-*sn*-glycero-3-phosphocholine (DOPC) and cholesterol were from Avanti Polar Lipids (Alabaster, AL). 7-Dehydrocholesterol, ergosterol, and cholesteryl acetate were from Fluka Chemie. 5-Cholesten-3-one was purchased from Aldrich. Lanosterol, β-sitosterol, and streptolysin were purchased from Sigma (St. Louis, MO). M344 monoclonal antibody was produced as described in ref *35*. Biotinylated anti-HA antibody was from HISS-Diagnostics (Freiburg, Germany), and streptavidin-phyco-erythrin (streptavidin-PE) was from Jackson Immunoresearch Laboratories (Hamburg, Germany). All other chemicals were from Sigma unless stated otherwise.

Listeriolysin Preparation. Hemagglutinin (HA)-tagged listeriolysin (LLO) was produced as described by Darji et al. (*35*). The hemagglutinin tag (YPYDVPDYA) is inserted

between amino acids 27 and 28 of the native LLO. Purified LLO was aliquoted and stored at −20 °C. An extinction coefficient, $\epsilon^{0.1\%}$, of 1.269 was calculated from the sequence at the ExPASy Proteomics tools Internet site (http://www.expasy.ch/tools/). LLO was always preincubated for at least 15 min on ice in a final dithiothreitol (DTT; Sigma) concentration of 10 mM, before any of the tests described below were performed. When needed, blanks with DTT alone were performed the same way as LLO experiments and were used for signal correction due to DTT effects.

Calcein Release. Large unilamellar vesicles (LUV) were prepared by extrusion of multilamellar vesicles. Lipids, dissolved in chloroform at a desired molar ratio of DOPC and cholesterol, were spread on the round-bottom glass flask on a rotary evaporator and dried under vacuum for at least 3 h. The lipid film was resuspended in 1 mL of approximately 60 mM calcein in 140 mM NaCl, 20 mM Tris-HCl (pH 8.5), and 1 mM EDTA (vesicle buffer) and frozen and thawed six times. Multilamellar vesicles were extruded through polycarbonate membranes with 100 nm pores by an Avestin lipid extruder (Avestin, Ottawa, ON) to yield LUV 100 nm in diameter (*36*). The excess of calcein was removed by gel filtration on a small G-50 column. The concentration of lipids was determined via an enzymatic test as described below. Permeabilization of calcein-loaded LUV was assessed by using a fluorescence microplate reader (Anthos Labtec Instruments GmbH). LLO was 2-fold diluted in vesicle buffer in a 96-well microtiter plate. One hundred milliliters of calcein-loaded LUV was added to each well to yield a final volume of 200 μL. The final concentration of lipids was 20 μM. The excitation and emission filters were set to 485 and 535 nm, respectively. The kinetics was followed for 52 min. The permeabilization induced by LLO was expressed as the percentage of the maximal permeabilization obtained at the end of the assay by the addition of detergent Triton X-100 to a final concentration of 2 mM in each well.

Surface Plasmon Resonance. Surface plasmon resonance (SPR) measurements were performed on a Biacore X (Biacore, Uppsala, Sweden) apparatus at 25 °C. An L1 chip was equilibrated in appropriate buffer, usually 20 mM Tris-HCl, 140 mM NaCl, and 1 mM EDTA (pH 8.5). The liposome-coated chip surface was prepared as described by Anderluh et al. (*37*). LUV were injected at a lipid concentration of 0.5−2 mM across the chip for 10 min at a rate of 1 μL/min. Loosely bound LUV were washed from the surface of the chip by two injections of 100 mM NaOH for 1 min at a rate of 30 μL/min. To test for the full coverage of the chip with the liposomes and to block the remaining nonspecific binding sites, 0.1 mg/mL bovine serum albumin (BSA) was injected once for 1 min at a rate of 30 μL/min. Erythrocyte ghosts were immobilized by using the same protocol to a final value of 1200 RU. LLO was injected over these prepared surfaces at the desired concentration for 90 s at a rate of 30 μL/min, and the dissociation was followed for 3 min. LLO was diluted to the appropriate concentration in a running buffer from a concentrated stock preincubated with 10 mM DTT. Blank injections were subtracted from sensorgrams to correct for the contribution of buffer and DTT to the increase of the response. Association and dissociation rate constants were globally fitted to a two-step binding model by using BIAevaluation version 3.2 (Biacore AB).

For membrane binding, this model usually assumes an initial surface binding step followed by a conformational change, which sometimes results in a protein stably inserted into the membrane (*38*). In our case, the second step represents aggregation of LLO monomers on the membrane surface (see also Discussion). The first 10 s of the injection and of the dissociation were not included in the fit due to refractive index effects.

Surface Pressure Measurements. Surface pressure measurements were performed with a MicroTrough-S system from Kibron (Helsinki, Finland) at room temperature under constant stirring. The aqueous subphase consisted of 500 μL of buffer, usually 10 mM Hepes and 200 mM NaCl (pH 7.5). Appropriate lipid mixtures, dissolved in chloroform and methanol (2:1, v:v), were gently spread over the subphase to create a monolayer. By changing the amount of lipid applied to the air–water interface, we attained the desired initial surface pressure. After incubation for 10 min, to allow for solvent evaporation, LLO was injected through a hole connected to the subphase. The final LLO concentration in the well was 0.3 μM. The increment in surface pressure versus time was monitored for more than 30 min.

Hemolysis Assay and Preparation of Erythrocyte Ghosts. Hemolysis of human red blood cells was assessed by using a microplate reader (MRX, Dynex) as described previously (*39*). Briefly, blood collected from healthy donors was washed a few times with 130 mM NaCl and 20 mM Tris-HCl (pH 7.4) (erythrocyte buffer). A suspension of erythrocytes was prepared to yield a final A_{630} of 0.5. LLO was 2-fold diluted in a final 100 μL of erythrocyte buffer. A suspension of erythrocytes was added to each well and hemolysis monitored at 630 nm for 20 min at room temperature. The final volume in each well was 200 μL.

Erythrocyte ghosts were prepared from washed erythrocytes by lysing 50 μL of erythrocytes with 1400 μL of cold 5 mM Na_2HPO_4 (pH 8.0) for 5 min on ice. Lysed erythrocytes were collected on the bottom of the microtube by centrifugation in a benchtop microcentrifuge for 10 min at 16100g. Erythrocyte ghosts were washed with the same buffer until all the hemoglobin was washed away, i.e., until no red color was visible in the pellet. The pellet was resuspended in a small volume of 140 mM NaCl, 20 mM Tris-HCl (pH 8.5), and 1 mM EDTA. Cholesterol was depleted from erythrocytes by methyl-β-cyclodextrin incubation; washed erythrocytes (0.5 mL) were incubated in 10 mM methyl-β-cyclodextrin in a final volume of 5 mL for 30 min at 37 °C. Erythrocytes were washed well before use in the hemolytic assay or ghost preparations. The removal of cholesterol from erythrocyte membranes was confirmed by enzymatic tests for lipid concentration determination of phospholipids B (for choline-containing lipids) and free cholesterol C (for cholesterol) (both from Wako). Additionally, thin layer chromatography of total lipid extracts was carried out to confirm removal of cholesterol and to show that the amounts of other lipids in the membrane were unchanged.

Flow Cytometry. LLO was added to J774 cells to a concentration of 1 μg/mL, and the cells were incubated for 10 min on ice. Thereafter, cells were washed in ice-cold PBS and then stained with the monoclonal anti-HA-biotin (1:2000) followed by streptavidin-PE staining. Cells were analyzed using a FACS-Calibur flow cytometer and Cell Questpro

(Becton Dickinson). Propidium iodide uptake was used to estimate cell viability. To remove cholesterol in the membranes of J774 cells, cells were incubated with filipin (100 μg/mL) for 1 h at 37 °C in serum-free medium.

RESULTS

Binding of LLO to Immobilized Liposomes. In this study, we have performed a detailed characterization of LLO binding and pore formation using surface plasmon resonance (SPR), insertion in lipid monolayers, and calcein release experiments to provide insight into the binding of LLO to lipid membranes. SPR, in particular, has proven to be a valuable experimental approach in the studies of protein membrane binding (*40*−*42*). Liposomes are immobilized on the surface of the sensor chip, and the protein of interest is passed across them. The increase in the magnitude of the signal is proportional to the concentration of the protein close to the surface of the sensor chip. We chose the L1 chip, which contains a dextran matrix with lipophilic alkyl chains that act as anchors to capture intact liposomes (*37*, *43*). In principle, this chip can also be used to study on-chip permeabilization of immobilized liposomes by membrane-damaging agents (*37*). We have initially performed SPR experiments using liposomes composed of phosphatidylcholine with unsaturated acyl chains, i.e., 1,2-dioleoyl-*sn*-glycero-3-phosphocholine (DOPC) and various amounts of cholesterol. DOPC was chosen, as there should not be any nanometer to micrometer lipid domain formation or phase separation in the cholesterol concentration range that was employed, i.e., 0−50% (molar ratio) (*44*, *45*). Therefore, there should not be any significant interference to the binding of LLO due to the changed physical state of the membrane; instead, the binding should be affected only by the amount of its lipid receptor. The L1 chip was fully covered with liposomes to a level of around 11 000 resonance units (RU). The complete surface coverage was indicated by an absence of any BSA binding (*37*, *43*). All experiments were performed within a LLO concentration range of 5−50 nM. At these concentrations, we did not always reach the saturation of binding during the association phase required for proper subsequent kinetic data analysis (*46*). Low LLO concentrations were chosen to minimize contributions of later steps in the pore-forming mechanism to the binding, i.e., aggregation of monomers on the surface of the membrane. However, as described in more detail below, this still did not completely prevent functional pore formation.

LLO binding showed pH and cholesterol dependence in such a system (Figure 1). LLO bound poorly to pure DOPC liposomes, with a slight increase in the the level of binding at pH 6.5 (Figure 1A) compared to that at pH 8.5 (Figure 1B). This is in agreement with Jacobs et al. (*47*), who observed weak binding of LLO to phosphatidylcholine liposomes via SDS−PAGE. This unspecific binding was nevertheless negligible compared with binding of LLO to liposomes containing 20% cholesterol (panels C and F of Figure 1 for pH 6.5 and 8.5, respectively). Binding to cholesterol-containing membranes was strongest at lower pH values, i.e., 5.5 and 6.5 (panels C and D of Figure 1, respectively). Under these conditions, no saturation of the binding was observed during 90 s of the association phase at any of the LLO concentrations that were applied. The binding resulted in a stably membrane-associated protein with
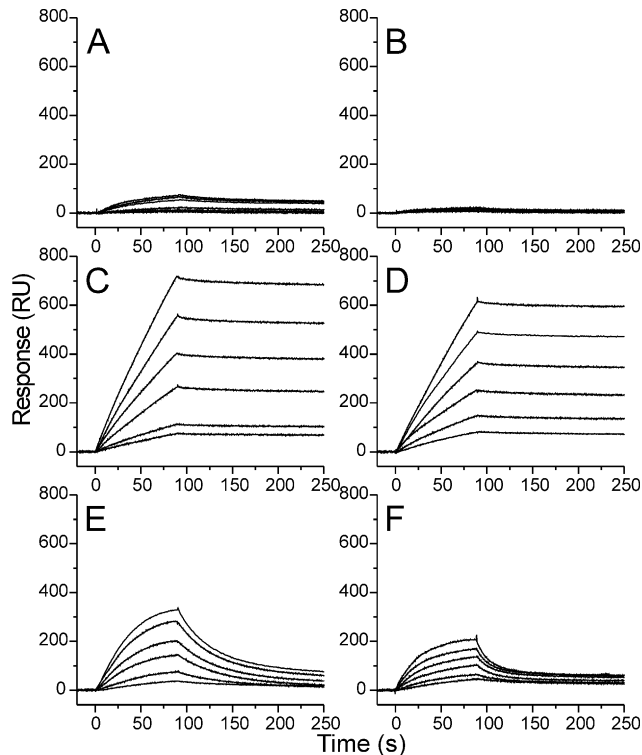
FIGURE 1: Binding of LLO to supported liposomes at different pH values. Liposomes were immobilized on the surface of the L1 chip to give approximately 11 000 RU. The flow rate was 30 μL/min. The association was followed for 90 s and the dissociation for 180 s. The running buffer was composed of 140 mM NaCl, 20 mM Tris-HCl (pH 8.5), and 1 mM EDTA. The concentrations of LLO were 5, 10, 20, 30, 40, and 50 nM (curves from bottom to top) in all cases: (A) DOPC liposomes at pH 6.5, (B) DOPC liposomes at pH 8.5, (C) DOPC/CHO-20% liposomes at pH 5.5, (D) DOPC/CHO-20% liposomes at pH 6.5, (E) DOPC/CHO-20% liposomes at pH 7.5, and (F) DOPC/CHO-20% liposomes at pH 8.5.

no desorption of LLO during the dissociation phase. There was less binding when the pH was increased; curves started to saturate, and binding was reversible, with most if not all LLO being desorbed from the surface of liposomes (Figure 1E,F). When binding was tested at high pH (pH 8.5) and a higher cholesterol concentration (35%), binding was found to be similar to that observed at pH 5.5 or 6.5 and lower cholesterol concentrations (i.e., 20%; Figure 2A). We next scanned the whole cholesterol concentration range at pH 8.5. Sensorgrams showed a clear cholesterol dependence of binding (Figure 2C), with a dramatic increase in the level of stably bound LLO at cholesterol concentrations higher than 35%. Up to this concentration, the binding was mostly reversible. Thus, the extent of binding and stabilization of LLO on liposomes is dependent in a nonlinear fashion on cholesterol content such that maximal binding occurs only once a threshold in cholesterol content is exceeded.

Curves in panels C and D of Figure 1 and Figure 2A are typical for a mass-transport effect (*46, 48*). When the amount of ligand on the surface of the chip, in our case cholesterol, is high, then the analyte cannot be delivered efficiently to saturate the ligand. To check for this possibility, we performed one of the suggested controls (*46*), i.e., binding of LLO to immobilized liposomes at different flow rates (8, 15, 30, and 60 μL/min), as there should be no differences in association in the absence of a mass-transfer effect. For the above-mentioned figures, a clear flow rate dependence was
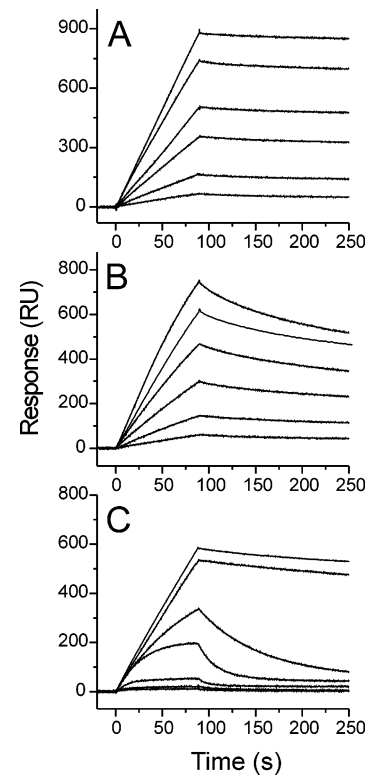

FIGURE 2: Binding of LLO to supported liposomes at pH 8.5. (A) Approximately 11 000 RU of DOPC/CHO-35% liposomes was immobilized on the L1 chip. (B) Approximately 1500 RU of DOPC/CHO-35% liposomes was immobilized on the L1 chip. The conditions and LLO concentrations used in panels A and B were the same as those described in the legend of Figure 1. (C) Binding of 40 nM LLO to liposomes of various cholesterol content: 0, 10, 20, 25, 30, 35, 40, and 45% cholesterol (from bottom to top).
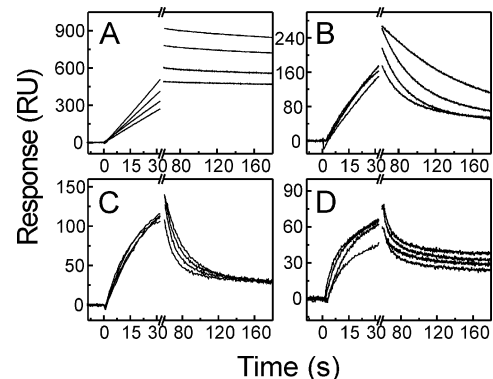

FIGURE 3: Binding of 50 nM LLO at different flow rates. Liposomes were immobilized on the surface of the L1 chip. The flow rates were 8, 15, 30, and 60 μL/min (from top to bottom). The association was followed for 60 s and the dissociation for 180 s. The running buffer was composed of 140 mM NaCl, 20 mM Tris-HCl (pH 8.5), and 1 mM EDTA. The concentration of LLO was 50 nM in all cases: (A) DOPC/CHO-35% liposomes at pH 8.5 and 11 000 RU, (B) DOPC/CHO-30% liposomes at pH 8.5 and 11 000 RU, (C) DOPC/CHO-20% liposomes at pH 8.5 and 11 000 RU, and (D) DOPC/CHO-30% liposomes at pH 8.5 and 1500 RU.

observed (Figure 3A). One of the solutions to avoid a mass-transfer effect is to reduce the concentration of the ligand on the surface of the chip. In our experimental setup, this can be done in two ways. Either liposomes with a low cholesterol content (20%) are immobilized on the chip, or the chip is only partially saturated but with liposomes with a high cholesterol content (>30%). Mass transfer was
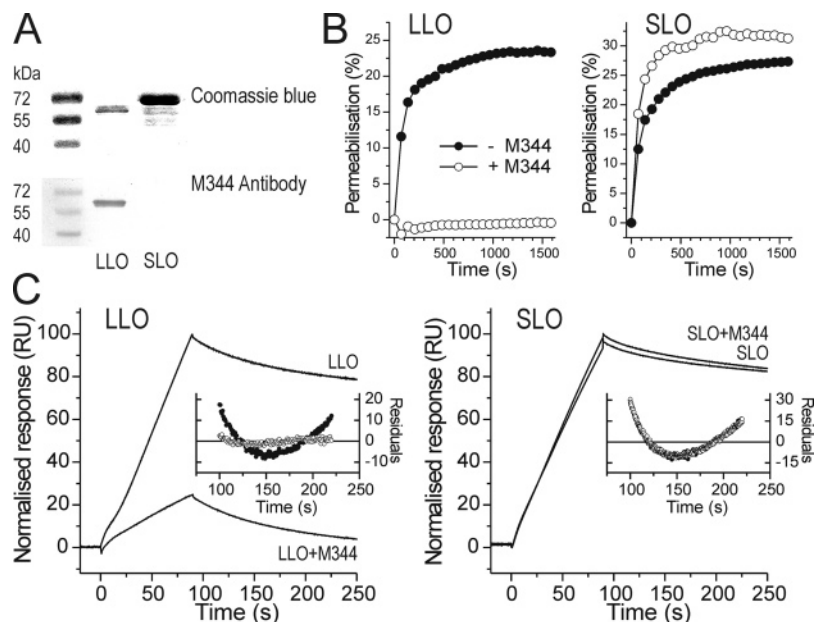
FIGURE 4: Effect of M344 antibody on LLO binding. (A) Approximately 1 μg of LLO or streptolysin was run on a 15% SDS−PAGE gel. The gel was stained with Coomassie blue (top panel) or blotted with M344 antibody and secondary goat anti-mouse antibody conjugated with horseradish peroxidase (bottom panel). (B) Release of calcein from DOPC/CHO-35% liposomes. The buffer used was composed of 140 mM NaCl, 20 mM Tris-HCl (pH 8.5), and 1 mM EDTA. The concentration of lipids was 40 μM. Approximately 0.15 μg of LLO or streptolysin was preincubated with 80 μg of M344 antibody for 30 min at room temperature. Liposomes were than added, and the time course of fluorescence was measured with a microplate reader and compared to controls without M344. The maximal release was determined at the end of the assay by addition of a final Triton X-100 concentration of 2 mM. (C) Approximately 100 nM LLO or streptolysin was preincubated with 80 μg of M344 antibody for at least 20 min at room temperature and than injected across immobilized DOPC/CHO-35% liposomes in the same buffer used for the calcein release experiment in panel B. Sensorgrams were corrected for the binding of M344 antibody alone. The inset shows residuals for the fit of the dissociation phase to a 1:1 Langmuir model. Panels B and C: (○) presence of M344 antibody and (●) absence of M344 antibody.

eliminated completely when liposomes with 20% cholesterol were used at the full chip coverage (Figure 3C). At 30% cholesterol, the association was not dependent on the flow rate, but dissociation still was [due to rebinding of analyte to the ligand at flow rates of 8 and 15 μL/min (Figure 3B)]. Mass transfer was also eliminated when the chip was only partially covered with liposomes that contained 30% cholesterol (Figure 3D). Figure 2B is one such example, where LLO binding was tested on high-cholesterol vesicles (35%) but at low chip coverage (approximately 1500 RU of lipids). In this case, curves start to saturate during the association phase and LLO is desorbed more efficiently (compare to Figure 2A, where the chip was fully covered with liposomes containing 35% cholesterol). As an important control, the binding of 25 nM LLO to the L1 chip alone was checked and found to be negligible.[2] That was an important control to check, because when the dextran layer with hydrophobic anchors is partially exposed the analyte may bind to them, and this can complicate data analysis.

The nonlinear dependence of binding on cholesterol concentration indicates that the binding is complex and that other steps in the pore-forming process may be involved, i.e., in plane aggregation of LLO. The following experiments were performed to check for these.

Oligomerization Promotes Stable Binding of the Toxin. The M344 monoclonal antibody that binds to the LLO linear epitope LTLSIDLP (LLO sequence 152−159) within domain 1 was reported to inhibit cytolysis of eukaryotic cells by blocking LLO oligomerization (26, 35). M344 specifically recognizes LLO, but not streptolysin, a CDC homologue from *S. pyogenes*, which was used as a control (Figure 4A). The presence of M344 blocked LLO permeabilizing activity on calcein-loaded liposomes (Figure 4B), in agreement with the reported inhibition of hemolytic activity (35). As expected, streptolysin was not affected by M344 preincubation (Figure 4B). LLO still binds significantly to immobilized LUV containing 35% cholesterol when preincubated with M344, despite the blocked permeabilizing activity. Again, M344 did not have any effect on the binding of streptolysin (Figure 4C). The dissociation phase of all sensorgrams was fitted to a monoexponential decay (Figure 4C, inset). A reasonable fit with a low χ^2 value (1.5) was obtained only for LLO preincubated with M344. The dissociation rate constant was 10.9×10^{-3} s^{-1}. This suggests that the dissociation is due to monomeric LLO. Large increases in the extent of binding in the absence of antibody may be explained by the formation of oligomers on the surface of the liposomes that depletes the monomeric bound form. Oligomers are more stably bound and desorb slowly in the dissociation step. In agreement, dissociation rate constants were 1 order of magnitude smaller than that for LLO preincubated with M344 and were 1.4×10^{-3}, 1.0×10^{-3}, and 0.9×10^{-3} s^{-1} for LLO, streptolysin, and streptolysin preincubated with M344, respectively. However, all these samples exhibited large deviations from the monoexponential fit (Figure 4C, inset), i.e., χ^2 values of 35.5, 84.8, and 88.9 for LLO, streptolysin, and streptolysin preincubated with M344, respectively. Data clearly show that

---

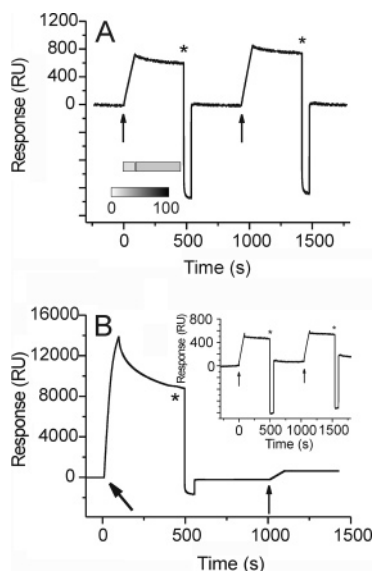[2] A. Bavdek and G. Anderluh, data not shown.

FIGURE 5: Desorption of bound LLO from liposomes. LLO was bound to immobilized calcein-loaded DOPC/CHO-45% liposomes at pH 8.5. Other conditions are as described in the legend of Figure 2. Bound LLO was completely desorbed from liposomes by a single injection of 100 mM NaOH for 60 s (asterisk). (A) Binding of 50 nM LLO (arrow). The buffer from the chip was collected during the association and dissociation phases and the fluorescence measured in a fluorimeter. It is shown below the trace. (B) Binding of 1 mM LLO (large arrow). After the NaOH wash, the surface was probed again with the injection of 50 nM LLO (small arrow). The inset shows the binding and removal of approximately 50 nM streptolysin.

the dissociation of LLO and streptolysin from membranes with a high cholesterol content is a slow but complex process composed of several steps.

How Stable Is "Stably Bound" Toxin? We could regenerate the liposome surface during SPR experiments at any pH or cholesterol concentration by desorbing LLO from the liposomes with a brief 1 min wash with 100 mM NaOH. High pH is usually used to desorb superficially bound peripheral proteins. One injection of NaOH was sufficient to remove 50 nM LLO, the highest concentration used in experiments presented in Figures 2−4 (Figure 5A). As SPR reports the change in mass concentration on the surface of the chip, desorbed material could be LLO, lipids, or complexes of both. However, the binding of LLO subsequently injected was the same as during the first injection (Figure 5A), indicating that no liposomes were desorbed and that the liposome surface remained intact during the LLO binding and regeneration. Although we cannot exclude the possibility that individual lipid molecules bound to LLO are extracted during the regeneration, larger proteolipid complexes, such as those observed for pneumolysin (49), were unlikely to be formed under our conditions.

It is possible to estimate the number of liposomes on the chip surface, and also the amount of bound LLO on a single vesicle, by assuming that 1000 RU corresponds roughly to 1 ng of matter (lipid or protein) per 1 mm^2 in a Biacore setup (see also ref 37). Approximately 700 RU of bound LLO after dissociation for 5 min using the conditions in Figure 5A would then correspond to approximately 65 molecules of LLO per single liposome. This is theoretically enough to form up to two complete transmembrane pores, but most likely the bound and then eluted LLO is a mixture

of a monomeric form, oligomers composed of few monomers, and pores.

The same regeneration was observed when the concentration of LLO was 20 times higher (1 μM). In this case, the amount of bound LLO after dissociation for 5 min was more than 8000 RU (Figure 5B), which gives approximately 700 molecules per liposome. This should drive the pore formation to its final stages or at least significantly increase the amount of stably inserted final complete pores. But, surprisingly, also in this case, bound LLO was completely desorbed with a single injection of NaOH (Figure 5B), indicating that association of LLO with liposomes is not particularly stable in any stage of pore formation. Hence, most of the toxin is bound to the surface of the membrane under these conditions but partially inserted; i.e., only a few stable transmembrane pores are present.

The high-pH wash could in principle reverse the effect of low pH on LLO structure and, consequently, decrease its affinity for cholesterol in membranes. To test for this possibility, we checked the binding and desorption of streptolysin, a CDC member that does not exhibit pH dependence of activity. However, also in the case of streptolysin, almost complete desorption of a stably bound toxin was achieved with a single NaOH injection (Figure 5B, inset). SPR experiments thus provide a unique observation that membrane-bound forms of CDC are not very stably inserted in the lipid bilayer in oligomeric, prepore, or pore states.

Permeabilizing Activity. It is possible to semiquantitatively estimate the permeabilizing activity of PFT on immobilized liposomes (37). To this end, liposomes loaded with the fluorescent probe calcein were immobilized on the surface of the L1 chip. The buffer eluted from the surface of the flow cell was collected during LLO association and dissociation stages, and the fluorescence was measured and compared to what remained on the chip and was eluted at the end of the experiment by the 2:3 (molar) mixture of 2-propanol and NaOH (Figure 5A, inset). This experiment was initially performed as a control to show that under the conditions described in the legend of Figure 5A no calcein is released from the liposomes, as there should not be enough monomers on the surface of a single liposome to efficiently form large pores. However, the calcein leakage was substantial. At 50 nM LLO, 19.8 ± 7.1% (n = 3, average ± standard deviation) of the calcein was released from the surface of the chip in the association phase and a further 25.7 ± 4.8% was released during the dissociation phase, yielding a final level of release of 45.6 ± 6.2% (Figure 5A). During the dissociation phase, the surface of the chip is flushed with the running buffer and liposomes are not in contact with fresh LLO. Hence, the high level of calcein release observed in the dissociation is unexpected and hints at rearrangements of bound LLO on the surface of liposomes leading to the formation of functional pores. In comparison, we have not observed this kind of behavior with equinatoxin II, a pore-forming toxin from sea anemones. Equinatoxin II rapidly forms the final pore state as all of the calcein release was observed in the association phase and none in the dissociation phase (37).

We next performed experiments with release of calcein from liposomes in solution at high pH 8.5 and at various cholesterol concentrations (Figure 6). LLO released calcein
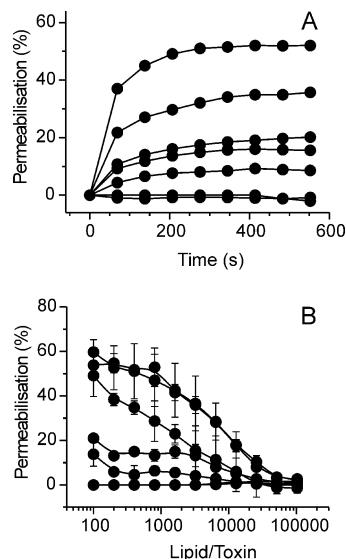
FIGURE 6: Calcein release. Calcein release was assessed with a microplate reader in 140 mM NaCl, 20 mM Tris-HCl (pH 8.5), and 1 mM EDTA. The concentration of lipids was 20 μM. The maximal level of release was determined at the end of the assay by addition of a final Triton X-100 concentration of 2 mM. (A) Time courses of the release of calcein from vesicles with various cholesterol contents (0, 10, 20, 30, 35, 40, and 50% cholesterol from bottom to top). The lipid:LLO ratio was 800. (B) Permeabilization at different lipid:toxin ratios for liposomes with various cholesterol contents (0, 10, 20, 30, 35, 40, and 50% cholesterol from bottom to top). $n = 2$ (average $\pm$ standard deviation).

in a cholesterol-dependent manner with the most effective release occurring when more than 35% of cholesterol was in the membrane (Figure 6A). The release was also dependent on the concentration of LLO. There was a gradual continuous increase in the level of permeabilization when the LLO concentration was increased and did not reach 100% even at a lipid:toxin (L:T) ratio of 100. At high cholesterol concentrations, i.e., 40 and 50%, significant release, approximately 20%, was observed even at an L:T ratio of 12 800. Under these conditions, the amount of LLO per liposome is not enough to form a complete pore, i.e., approximately eight molecules per liposome. It is possible that, at the low concentrations of LLO used here, in addition to pore formation other mechanisms may interfere with calcein release. The binding of the toxin molecule to the surface of the liposome could destabilize the membrane or trigger a lipid rearrangement that would result in the observed low level of calcein release, similar to the carpetlike mechanism observed for shorter peptides (50).

The result of on-chip permeabilization (approximately 46%) is in agreement with the result of permeabilization performed with liposomes in a solution. At an L:T ratio of 1600, corresponding to an L:T ratio of approximately 1400 for on-chip conditions, the level of release was 43% (the average of two independent measurements).

LLO Inserts into Lipid Monolayers in a pH- and Cholesterol-Interdependent Fashion. Insertion of LLO in lipid monolayers was used as a technique complementary to SPR. We initially investigated insertion of LLO at the water–air interface (Figure 7A). An increase of ~12 mN/m was observed at LLO concentrations above 0.3 μM, indicating that LLO has an amphipathic character. LLO can also insert into DOPC lipid monolayers when cholesterol is present
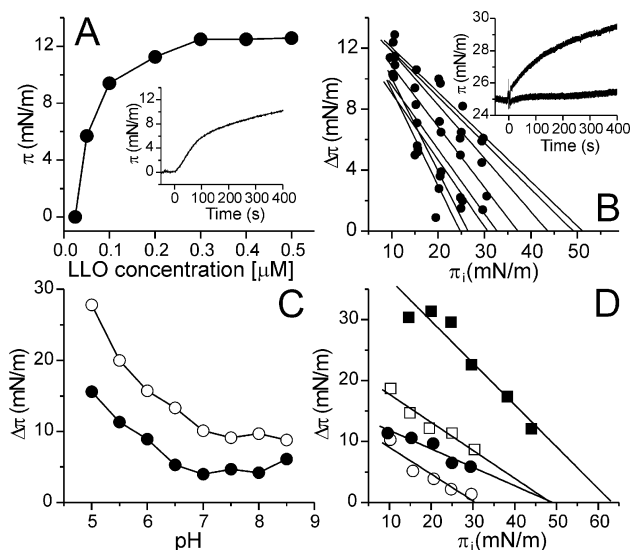

FIGURE 7: Insertion of LLO into lipid monolayers. The concentration of LLO was always 0.3 μM in 200 mM NaCl and 10 mM HEPES (pH 7.5). (A) Insertion of LLO into the air–water interface. The inset shows the time trace of 0.3 μM LLO insertion. (B) Critical pressure plots for monolayers with various cholesterol contents (0, 10, 20, 25, 30, 35, 40, and 45% from left to right). The inset shows the time trace of insertion of LLO into a DOPC monolayer (bottom trace) or a DOPC/CHO-35% monolayer (top trace) at an initial pressure of 25 mN/m. Other conditions are as described for panel A. (C) Increase in surface pressure after insertion of LLO into DOPC/CHO-20% (●) and DOPC/CHO-40% (○) monolayers at various pH values. The initial pressure was 20 mN/m. Other conditions are as described for panel A. (D) Critical pressure plots for insertion of LLO into DOPC/CHO-40% monolayers at pH 7.5 (●) and 5.5 (■) and DOPC/CHO-20% monolayers at pH 7.5 (○) and 5.5 (□). Other conditions are as described for panel A.

(Figure 7B). No insertion was observed when a monolayer of DOPC was used, but when cholesterol was present, a significant increase was observed even at pH 7.5 (Figure 7B, inset). The kinetics of insertion was not monoexponential; most likely, not only was insertion of the monomer observed, but other steps of the pore-forming mechanism (i.e., aggregation) also contributed to the signal. We constructed a critical pressure plot from the increase in surface pressure upon LLO insertion measured at various initial pressures (Figure 7B). Various cholesterol concentrations were compared at pH 7.5. Critical pressures, i.e., pressures at which no insertion of LLO occurs, were determined from extrapolated data and are summarized in Figure 10. They ranged from 24.7 mN/m for DOPC monolayers to 51.6 mN/m when 45% cholesterol was present. The critical pressure in natural membranes is ~30 mN/m (51, 52). In the case of LLO, this value was exceeded when 25% cholesterol was present (critical pressure of 32.9 mN/m).

The pH dependence of insertion was determined at two cholesterol concentrations, i.e., 20 and 40% (Figure 7C). At both concentrations, the insertions were better at acidic pH values, while there was no change in insertion between pH 7 and 8.5. The critical pressure for 20% cholesterol at pH 7.5 was 30.5 mN/m. When the pH was lowered to 5.5, the critical pressure increased to 48.5 and was strikingly similar to the critical pressure when 40% cholesterol was present at a higher pH (7.5). When a low pH (5.5) and high cholesterol concentration (40%) were used, the critical pressure was 63.5. LLO clearly needs a low pH for efficient insertion at low cholesterol concentrations, but when the pH is increased, the
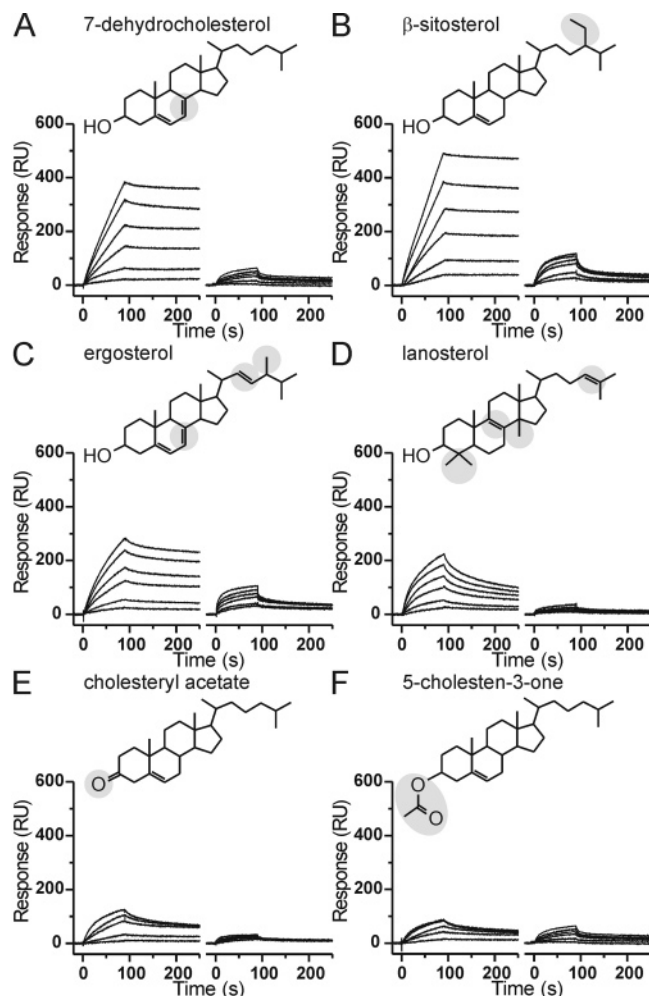
FIGURE 8: Binding of LLO to supported liposomes containing various sterols. All conditions are as described in the legend of Figure 1. In all cases, liposomes composed of DOPC contained 20% various sterols (by moles). For each sterol, the left panel shows binding at pH 6.5 and the right panel shows binding at pH 8.5. The changes from cholesterol structure are shaded on sterol chemical formulas. The concentrations of LLO were in all cases 5, 10, 20, 30, 40, and 50 nM (curves from bottom to top): (A) 7-dehydrocholesterol, (B) β-sitosterol, (C) ergosterol, (D) lanosterol, (E) cholesteryl acetate, and (F) 5-cholesten-3-one.

same insertion is observed at higher cholesterol concentrations. This is in agreement with SPR binding data.

The Binding of LLO to Liposomes Containing Other Sterols. To test the specificity of LLO in binding to cholesterol, we have studied the binding to liposomes where cholesterol was replaced by various other sterols (Figure 8). Sterols chosen were such that the changes in the chemical structure were rather small, as in the case of 7-dehydrocholesterol or β-sitosterol, that they were located in the ring system, as in the case of ergosterol or lanosterol, or that the 3β-hydroxy group was changed, as in the case of cholesteryl acetate or 5-cholesten-3-one. As is evident from sensorgrams in Figure 8, the binding of LLO to liposomes when 7-dehydrocholesterol or β-sitosterol was present at 20% in DOPC liposomes was highly similar to the binding when cholesterol was present in DOPC LUV, at both low and high pH (compare the data to Figure 1). The binding to cholesteryl acetate and 5-cholesten-3-one was poor at both pH values, while the binding to ergosterol or lanosterol showed intermediate levels between these two extremes. Binding to all

sterols showed a pH dependence; i.e., the binding at pH 6.5 was stronger than that at pH 8.5.

LLO Activity at Suboptimal pH on Cells. We finally checked whether LLO binds and permeabilizes cells at physiological or higher pH values. LLO bound readily to J774 cells at pH 7.4 and formed pores permeable to propidium iodide in 52% of the cells (Figure 9A,B). LLO at this pH retains cholesterol specificity, as preincubation of J774 cells with 100 μM filipin drastically decreased the level of binding. The cholesterol dependence of binding was further confirmed by SPR by using erythrocyte ghosts as a ligand. Ghosts were immobilized on the surface of an L1 chip at pH 8.5. LLO did not bind to ghosts prepared from cholesterol-depleted erythrocytes but exhibited significant binding to ghosts prepared from untreated erythrocytes (Figure 9C). The sensorgram that describes binding to untreated ghosts is qualitatively similar to sensorgrams of binding to liposomes at a high cholesterol concentration at pH 8.5 (Figure 2). Binding results correlated well with hemolytic activity; i.e., LLO was not active against cholesterol-depleted erythrocytes but readily lysed untreated erythrocytes (Figure 8D). The binding and hemolytic activity at higher pH values thus correlated with the amount of cholesterol in membranes. These results clearly show that LLO can exhibit typical CDC properties, cholesterol-dependent binding and permeabilizing activity, toward two different types of cells at physiological or even slightly basic pH values.

DISCUSSION

In this paper, we have studied the binding and permeabilizing activity of LLO at pH values that are not considered optimal but are nevertheless physiological. Experiments were performed on model lipid membranes and model cell systems. We provide important insights into the binding and permeabilizing activity of LLO and show that under suboptimal pH conditions LLO retained a significant ability to bind and form pores in lipid membranes. These results have important implications for the understanding of the mechanism of pore formation by CDC and *Listeria* pathogenesis.

Binding to Membranes Containing Cholesterol. It is interesting that the binding to DOPC membranes without cholesterol is negligible and that significant binding at either pH value occurs only in the presence of cholesterol (Figures 1 and 2). Obviously nonspecific adsorption, i.e., electrostatic interactions, plays only a minor role in LLO binding, whereas recognition of cholesterol is crucial and dramatically improves the binding. LLO thus clearly exhibits a cholesterol dependence, the most important property of CDC, at low and high pH values.

The data from three independent assays, SPR, lipid monolayers, and calcein release experiments, clearly indicate that, between 0.3 and 0.4 mole fraction cholesterol, a threshold and narrow transition from very low to high LLO binding and permeabilizing activities exist. The maximal effect is achieved above 0.4 mole fraction cholesterol (Figure 10). A similar threshold of around 40−50% cholesterol and a narrow transition from weak to strong binding were observed also for other CDC (*53−56*) and seem to be a general property. This effect is exemplified for LLO by comparison of the amount of LLO bound when the chip is fully covered with liposomes containing 20% cholesterol (Figure 1F) or
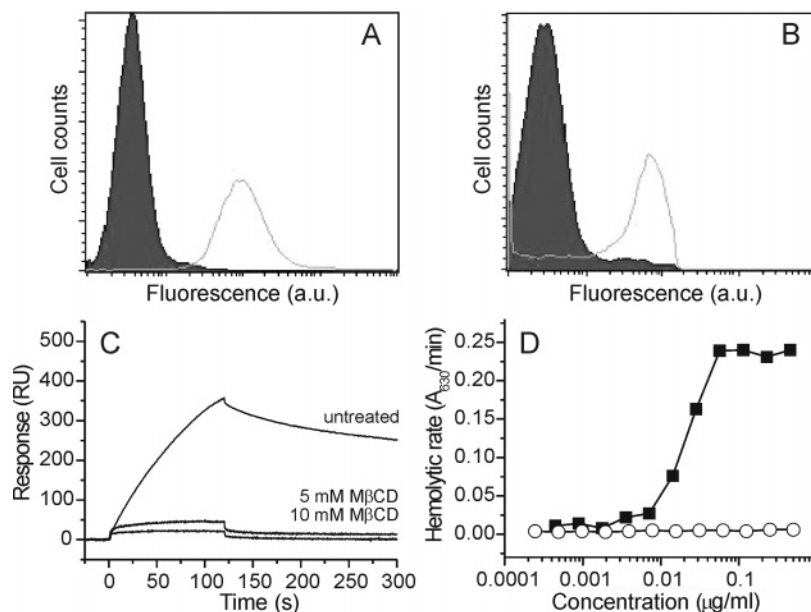
FIGURE 9: Binding of LLO to J774 cells and erythrocyte ghosts. (A) J774 cells were incubated with LLO on ice for 15 min at pH 7.4. After being washed, cells were stained with biotinylated anti-HA antibody followed by streptavidin-PE and analyzed by flow cytometry. Only viable cells (propidium iodide-excluding cells) were analyzed for the bound toxin. The LLO binding is represented as the relative fluorescence intensity. The shaded histograms show the background staining of the control cells not incubated with LLO. (B) Uptake of propidium iodide by J774 cells incubated with LLO exactly the same as described for panel A. (C) Binding of 25 nM LLO to erythrocyte ghosts assessed by SPR. Approximately 1200 RU of erythrocyte ghosts was immobilized on the surface of the L1 chip. The running buffer was composed of 140 mM NaCl, 20 mM Tris-HCl (pH 8.5), and 1 mM EDTA. The association was followed for 2 min at a rate of 30 μL/min. (D) Hemolytic activity of LLO toward human erythrocytes (■) or to erythrocytes with cholesterol depleted (○). Hemolytic activity was measured with a microplate reader in 130 mM NaCl and 20 mM Tris-HCl (pH 7.4) by monitoring the absorbance at 630 nm for 20 min. The maximal rate of hemolysis was determined from the traces.
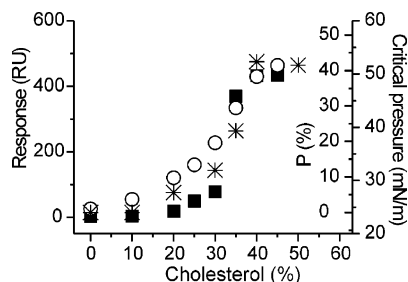

FIGURE 10: Summary of LLO experiments on model lipid systems. The amount of stably bound LLO after dissociation for 3 min as measured by SPR is shown as black squares; critical pressures for insertion of LLO in monolayers are shown as white circles, and the level of calcein release at an L:T ratio of 1600 is shown as asterisks.

when the chip is only partially covered with liposomes, but with a high (i.e., 35%) cholesterol content (Figure 2B). Although there is approximately 4 times more cholesterol on the chip in the former, binding is much better in the latter, indicating that the amount of cholesterol in each liposome is critical for stable binding and further steps of the pore-forming mechanism.

One of the most useful aspects of SPR is that it is able to provide kinetic constants for the binding process without the need for the labeling of the binding partners. Experimental conditions for rigorous kinetic analysis are sometimes difficult to achieve in protein membrane SPR; hence, we performed additional controls to determine the conditions in our study under which mass-transfer effects occurred (Figure 3) (*46, 48*). The most useful sensorgrams for kinetic analysis were, therefore, those that do not suffer from a mass-transfer effect, as observed in Figures 1F and 2B. We initially attempted to fit sensorgrams with dedicated software using

a 1:1 binding model. It gave overly high χ^2 values and was disregarded also on the basis of additional experiments that were performed (Figures 4 and 5). We, therefore, used the two-step model that assumes a change in the structure of the analyte after initial binding to the membrane (*38*). The second step does not contribute to the total signal but sometimes results, due to a structural change in a bound molecule, in a more stably bound protein. This is analogous to our case, where initially bound monomers reacted with other monomers or oligomers of LLO on the membrane, thus changing their kinetic properties. We assumed that interaction of the monomer with different-sized aggregates (e.g., dimers, trimers, tetramers, etc.) is identical. Although the fits to the data gave acceptable χ^2 values (Table 1), the results need to be interpreted with caution. Additional experiments described above showed that it might be necessary to account for more steps than mere simple binding of the monomer to the membrane and aggregation. Kinetic analysis of sensorgrams obtained when the chip was fully covered with liposomes with a low cholesterol content (curves from Figure 1F) or only partially covered but with a high cholesterol content (curves from Figure 2B) indicated that the association rate of both steps is largely unaffected by cholesterol content, but instead, large changes in dissociation rates were observed. These decreased, when a high cholesterol concentration was present in liposomes, ~6- and ~8-fold for the first and second phases, respectively (Table 1). These changes increased the equilibrium dissociation rate constant by more than 60. High cholesterol concentrations bring LLO monomers closer on the surface of the membrane and consequently enable their interaction with a stable oligomeric complex, while low cholesterol concentrations enable transient and

Table 1: Binding Constants for the Binding of LLO[a]

conditions	k_{a1} ($\times 10^4$ M^{-1} s^{-1})	k_{d1} ($\times 10^{-3}$ s^{-1})	k_{a2} ($\times 10^{-3}$ s^{-1})	k_{d2} ($\times 10^{-4}$ s^{-1})	K_{D1} ($\times 10^{-7}$ M)	K_{D2} ($\times 10^{-2}$)	K_D ($\times 10^{-9}$ M)	χ^2
20% cholesterol with 11 000 RU	4.3 ± 4.2	42.9 ± 5.2	8.1 ± 0.3	20.3 ± 10.7	17.6 ± 11.6	25.4 ± 14.1	345 ± 178	3.6−5.0
35% cholesterol with 1500 RU	7.1 ± 6.2	7.5 ± 6.0	6.3 ± 1.7	2.7 ± 2.9	1.7 ± 1.4	4.0 ± 2.3	5.5 ± 3.0	4.1−10.1
fold change	0.6	5.8	1.3	7.5	10.5	6.4	63.3	

[a] Binding constants were obtained after fitting the SPR data from Figures 1F and 2B to a two-step binding model with BIAevaluation version 3.2. Experimental conditions are described in the legend of Figure 1. $n = 3$ (average ± standard deviation).

largely reversible binding. This consequently increases the amount of bound LLO and decreases the rate of dissociation from the membrane. Cholesterol, therefore, not only increases the initial level of binding to the membrane but also significantly affected a subsequent aggregation step of monomers on the surface of the liposome; i.e., it prevented dissociation of monomers from oligomers. This is in agreement with a notion that when CDC oligomers are formed, they are remarkably stable structures and are even resistant to SDS (*17*).

High cooperativity of binding and activity with respect to cholesterol concentration in membranes indicates the importance of the lateral distribution and accessibility of cholesterol in membranes for LLO. Clustered cholesterol molecules (*57−59*) will form in lipid membranes when the cholesterol concentration is increased above a certain threshold, i.e., when the capacity of phospholipids to shield cholesterol from the aqueous media is exceeded (*60*). Such small clusters of cholesterol could serve as docking sites for LLO and facilitate oligomerization, as shown by our results. Clustered lipids as binding sites for proteins emerge as a general concept in PFT; i.e., the binding and permeabilizing activity of ostreolysin, a PFT from oyster mushroom, is optimal above 40% cholesterol in sphingomyelin-containing membranes (*61*), and Valeva et al. have recently shown that clustered phosphocholine headgroups lead to rapid oligomerization of staphylococcal α-toxin (*62*).

Sterol Specificity of LLO. The exact mechanism of binding of cholesterol by CDC is not yet known. It was suggested that CDC possess a binding site for cholesterol located close to the undecapeptide motif with exposed tryptophans on the large loop on the tip of domain 4 (*9*). Some fluorescence data exist to show that cholesterol specifically interacts with exposed tryptophans in that region (*63*). Binding of LLO to cholesterol was shown to proceed in a roughly 1:1 stoichiometry (*47*). The SPR approach allowed us to check the cholesterol specificity of LLO by using DOPC liposomes with 20% of various other sterols. We have used six different sterols, which have moderate to extensive changes from the chemical structure of cholesterol (Figure 8), and we have checked binding at low (6.5) and high (8.5) pH values. The results that we obtained allowed us to come to two clear conclusions. The LLO seems to specifically recognize the 3β-hydroxy group of cholesterol, as any changes to this region, as exemplified by lanosterol, cholesteryl acetate, and 5-cholesten-3-one structures (Figure 8), decreased the extent of binding significantly. Second, binding of LLO to any of the sterol structures was pH-dependent, amazingly even with those where the binding at pH 8.5 was negligible, i.e., cholesteryl acetate and 5-cholesten-3-one. This observation leads to the conclusion that the pH dependence of LLO is not related to the cholesterol recognition, but with other steps within the pore-forming mechanism. Our results thus clearly show that the specificity of LLO for cholesterol is limited to the most exposed hydrophilic part of the sterol molecule. Similar effects of sterol structure on binding or permeabilizing activity were observed for LLO and other CDC (*47*, *53*, *63−65*). Our and other results, therefore, show that a specific interaction between cholesterol and CDC exists. It is generally assumed that CDC bind cholesterol via domain 4. However, the fact that domains 1−3 can bind to cell membranes without domain 4 (*66*) suggests that LLO membrane binding is more complex than we have presumed.

Formation of Functional Pores by LLO. Results of on-chip permeabilization, permeabilization of liposomes in solution, and permeabilizing activity on cells clearly show that LLO is able to form pores at physiological and slightly basic pH. A gradual increase in the level of permeabilization with an increased LLO concentration indicates that complete large pores are not a prerequisite for calcein release, since it is released also under conditions where there is not enough LLO present on a single vesicle to form a single pore (Figure 6). In the case of perfringolysin, probably one of the best-studied PFT and CDC, a prepore model was formulated, in which only the final complete pores are permeable. Before that stage, perfringolysin oligomers remain as prepores but are not inserted into the membrane (*67*). However, this mode of action was recently questioned for other members of CDC (*8*), and the literature actually suggests that incomplete circular oligomers, so-called arcs, may be the functional entity for other members of CDC; i.e., arcs of streptolysin were shown to be functional (*68*) (although see also ref *67*). Our data are in agreement with this model and hint that smaller aggregates of LLO are actually functional. In this regard, it was interesting to observe that LLO, and streptolysin, in a liposome system are not so strongly inserted into the lipid bilayer at any of the stages of the pore-forming mechanism, since a single injection of 100 mM NaOH desorbs protein almost completely from the surface of liposomes, regardless of the amount of toxin bound to the membrane (Figure 5). This is unlike the final pore states of other PFT in the lipid bilayer which are remarkably stable structures; thus, it is often nearly impossible to remove them from the lipid membrane (*38*).

Although complete ring-structured pores by CDC are well-documented on erythrocytes or supported lipid membranes, it is not at all clear whether the toxin concentration necessary for complete oligomers can indeed be attained under physiological circumstances. Thus, the ability of LLO, or any CDC for that matter, to form incomplete, albeit functional pores from few monomers is consistent with the physiological realities. Indeed, the recent study by Shaughnessy et al. (*69*), showing that LLO caused successive release of small to large molecules from phagosomes, is in accordance with initial formation of small but growing oligomeric pores. This view

does not, however, exclude the possibility that LLO forms pores via a prepore complex. It is quite likely that different CDC members create pores by either mechanism, or a combination of both (*8*).

LLO Activity at "Suboptimal" pH. LLO is a multifunctional protein that not only mediates disruption of phagosomal membranes but also triggers cellular signals at the plasma membrane (*26*). What is the significance of binding of LLO to plasma membranes at physiological pH? LLO was shown to exert long distance effects by being involved in induction of apoptosis in T cells that are not directly infected by *L. monocytogenes* (*34*). Furthermore, we recently showed that *L. monocytogenes* strongly activates mast cells via LLO while remaining attached to the cells and without being phagocytosed.[3] Thus, binding of LLO to host cell membranes at physiological pH plays a major role during the course of infection of *L. monocytogenes*. The data presented constitute an illustrative model of how LLO is adapted for its function at such disparate subcellular sites. We show that the critical threshold of cholesterol concentration required for stable binding and cytolytic activity is contingent on pH. At physiological or slightly basic pH, LLO exhibits significant insertion (Figure 7), binding (Figure 2B), and permeabilizing activity (Figure 5) only at cholesterol concentrations exceeding 30−35%. Such concentrations are typically found in lipid rafts, membrane microdomains rich in cholesterol and sphingolipids. This is in agreement with the recent study showing that LLO preferentially binds to lipid rafts in J774 cells (*26*).

The amount of cholesterol in membranes gradually decreases along the endosomal pathway. In spite of this, LLO is still able to bind to membranes with a low cholesterol content at low pH (Figure 1C,D). It remains to be determined whether LLO structure remains unaltered at low or high pH values and whether pores with similar properties are formed. The critical pressure plots for 20% cholesterol at pH 5.5 and 40% cholesterol at pH 7.4 have the same critical pressure value, but the slopes are considerably different (Figure 7D), indicating that there actually might be two different processes involved. Thus, the discovery that LLO activity at low pH and low cholesterol concentrations resembles that at high pH and high cholesterol concentrations reveals a toxin perfectly adapted for its intracellular role in mediating escape of bacteria from the phagosomes as well as in triggering signals at the plasma membrane.

ACKNOWLEDGMENT

REFERENCES

1. Sheehan, B., Kocks, C., Dramsi, S., Gouin, E., Klarsfeld, A. D., Mengaud, J., and Cossart, P. (1994) Molecular and genetic determinants of the *Listeria monocytogenes* infectious process, *Curr. Top. Microbiol. Immunol. 192*, 187−216.
2. Kathariou, S., Metz, P., Hof, H., and Goebel, W. (1987) Tn916-induced mutations in the hemolysin determinant affecting virulence of *Listeria monocytogenes*, *J. Bacteriol. 169*, 1291−1297.
3. Portnoy, D. A., Chakraborty, T., Goebel, W., and Cossart, P. (1992) Molecular determinants of *Listeria monocytogenes* pathogenesis, *Infect. Immun. 60*, 1263−1267.
4. Portnoy, D. A., and Jones, S. (1994) The cell biology of *Listeria monocytogenes* infection (escape from a vacuole), *Ann. N.Y. Acad. Sci. 730*, 15−25.
5. Beauregard, K. E., Lee, K. D., Collier, R. J., and Swanson, J. A. (1997) pH-dependent perforation of macrophage phagosomes by listeriolysin O from *Listeria monocytogenes*, *J. Exp. Med. 186*, 1159−1163.
6. Portnoy, D. A., Auerbuch, V., and Glomski, I. J. (2002) The cell biology of *Listeria monocytogenes* infection: The intersection of bacterial pathogenesis and cell-mediated immunity, *J. Cell Biol. 158*, 409−414.
7. Tweten, R. K. (2005) Cholesterol-dependent cytolysins, a family of versatile pore-forming toxins, *Infect. Immun. 73*, 6199−6209.
8. Gilbert, R. J. (2005) Inactivation and activity of cholesterol-dependent cytolysins: What structural studies tell us, *Structure 13*, 1097−1106.
9. Rossjohn, J., Feil, S. C., McKinstry, W. J., Tweten, R. K., and Parker, M. W. (1997) Structure of a cholesterol-binding, thiol-activated cytolysin and a model of its membrane form, *Cell 89*, 685−692.
10. Jacobs, T., Cima-Cabal, M. D., Darji, A., Méndez, F. J., Vázquez, F., Jacobs, A. A., Shimada, Y., Ohno-Iwashita, Y., Weiss, S., and De los, T. (1999) The conserved undecapeptide shared by thiol-activated cytolysins is involved in membrane binding, *FEBS Lett. 459*, 463−466.
11. Gilbert, R. J., Jiménez, J. L., Chen, S. X., Tickle, I. J., Rossjohn, J., Parker, M., Andrew, P. W., and Saibil, H. R. (1999) Two structural transitions in membrane pore formation by pneumolysin, the pore-forming toxin of *Streptococcus pneumoniae*, *Cell 97*, 647−655.
12. Tilley, S. J., Orlova, E. V., Gilbert, R. J., Andrew, P. W., and Saibil, H. R. (2005) Structural basis of pore formation by the bacterial toxin pneumolysin, *Cell 121*, 247−256.
13. Polekhina, G., Giddings, K. S., Tweten, R. K., and Parker, M. W. (2004) Crystallization and preliminary X-ray analysis of the human-specific toxin intermedilysin, *Acta Crystallogr. D60*, 347−349.
14. Weis, S., and Palmer, M. (2001) Streptolysin O: The C-terminal, tryptophan-rich domain carries functional sites for both membrane binding and self-interaction but not for stable oligomerization, *Biochim. Biophys. Acta 1510*, 292−299.
15. Shimada, Y., Maruya, M., Iwashita, S., and Ohno-Iwashita, Y. (2002) The C-terminal domain of perfringolysin O is an essential cholesterol-binding unit targeting to cholesterol-rich microdomains, *Eur. J. Biochem. 269*, 6195−6203.
16. Ramachandran, R., Heuck, A. P., Tweten, R. K., and Johnson, A. E. (2002) Structural insights into the membrane-anchoring mechanism of a cholesterol-dependent cytolysin, *Nat. Struct. Biol. 9*, 823−827.
17. Shepard, L. A., Shatursky, O., Johnson, A. E., and Tweten, R. K. (2000) The mechanism of pore assembly for a cholesterol-dependent cytolysin: Formation of a large prepore complex precedes the insertion of the transmembrane β-hairpins, *Biochemistry 39*, 10284−10293.
18. Shepard, L. A., Heuck, A. P., Hamman, B. D., Rossjohn, J., Parker, M. W., Ryan, K. R., Johnson, A. E., and Tweten, R. K. (1998) Identification of a membrane-spanning domain of the thiol-activated pore-forming toxin *Clostridium perfringens* perfringolysin O: An α-helical to β-sheet transition identified by fluorescence spectroscopy, *Biochemistry 37*, 14563−14574.
19. Shatursky, O., Heuck, A. P., Shepard, L. A., Rossjohn, J., Parker, M. W., Johnson, A. E., and Tweten, R. K. (1999) The mechanism of membrane insertion for a cholesterol-dependent cytolysin: A novel paradigm for pore-forming toxins, *Cell 99*, 293−299.
20. Geoffroy, C., Gaillard, J. L., Alouf, J. E., and Berche, P. (1987) Purification, characterization, and toxicity of the sulfhydryl-activated hemolysin listeriolysin O from *Listeria monocytogenes*, *Infect. Immun. 55*, 1641−1646.
21. Glomski, I. J., Gedde, M. M., Tsang, A. W., Swanson, J. A., and Portnoy, D. A. (2002) The *Listeria monocytogenes* hemolysin has an acidic pH optimum to compartmentalize activity and prevent damage to infected host cells, *J. Cell Biol. 156*, 1029−1038.
22. Schuerch, D. W., Wilson-Kubalek, E. M., and Tweten, R. K. (2005) Molecular basis of listeriolysin O pH dependence, *Proc. Natl. Acad. Sci. U.S.A. 102*, 12537−12542.
23. Decatur, A. L., and Portnoy, D. A. (2000) A PEST-like sequence in listeriolysin O essential for *Listeria monocytogenes* pathogenicity, *Science 290*, 992−995.

[3] N. Gekara and S. Weiss, data not shown.

24. Coconnier, M. H., Lorrot, M., Barbat, A., Laboisse, C., and Servin, A. L. (2000) Listeriolysin O-induced stimulation of mucin exocytosis in polarized intestinal mucin-secreting cells: Evidence for toxin recognition of membrane-associated lipids and subsequent toxin internalization through caveolae, *Cell. Microbiol. 2*, 487−504.

25. Gekara, N. O., and Weiss, S. (2004) Lipid rafts clustering and signalling by listeriolysin O, *Biochem. Soc. Trans. 32*, 712−714.

26. Gekara, N. O., Jacobs, T., Chakraborty, T., and Weiss, S. (2005) The cholesterol-dependent cytolysin listeriolysin O aggregates rafts via oligomerization, *Cell. Microbiol. 7*, 1345−1356.

27. Repp, H., Pamukci, Z., Koschinski, A., Domann, E., Darji, A., Birringer, J., Brockmeier, D., Chakraborty, T., and Dreyer, F. (2002) Listeriolysin of *Listeria monocytogenes* forms Ca^{2+}-permeable pores leading to intracellular Ca^{2+} oscillations, *Cell. Microbiol. 4*, 483−491.

28. Dramsi, S., and Cossart, P. (2003) Listeriolysin O-mediated calcium influx potentiates entry of *Listeria monocytogenes* into the human Hep-2 epithelial cell line, *Infect. Immun. 71*, 3614−3618.

29. Wadsworth, S. J., and Goldfine, H. (2002) Mobilization of Protein Kinase C in Macrophages Induced by *Listeria monocytogenes* Affects Its Internalization and Escape from the Phagosome, *Infect. Immun. 70*, 4650−4660.

30. Dramsi, S., and Cossart, P. (2003) Listeriolysin O-Mediated Calcium Influx Potentiates Entry of *Listeria monocytogenes* into the Human Hep-2 Epithelial Cell Line, *Infect. Immun. 71*, 3614−3618.

31. Kuhn, M., and Goebel, W. (1994) Induction of cytokines in phagocytic mammalian cells infected with virulent and avirulent *Listeria* strains, *Infect. Immun. 62*, 348−356.

32. Nishibori, T., Xiong, H., Kawamura, I., Arakawa, M., and Mitsuyama, M. (1996) Induction of cytokine gene expression by listeriolysin O and roles of macrophages and NK cells, *Infect. Immun. 64*, 3188−3195.

33. Guzman, C. A., Domann, E., Rohde, M., Bruder, D., Darji, A., Weiss, S., Wehland, J., Chakraborty, T., and Timmis, K. N. (1996) Apoptosis of mouse dendritic cells is triggered by listeriolysin, the major virulence determinant of *Listeria monocytogenes*, *Mol. Microbiol. 20*, 119−126.

34. Carrero, J. A., Calderon, B., and Unanue, E. R. (2004) Listeriolysin O from *Listeria monocytogenes* Is a Lymphocyte Apoptogenic Molecule, *J. Immunol. 172*, 4866−4874.

35. Darji, A., Niebuhr, K., Hense, M., Wehland, J., Chakraborty, T., and Weiss, S. (1996) Neutralizing monoclonal antibodies against listeriolysin: Mapping of epitopes involved in pore formation, *Infect. Immun. 64*, 2356−2358.

36. MacDonald, R. C., MacDonald, R. I., Menco, B. P., Takeshita, K., Subbarao, N. K., and Hu, L. (1991) Small-volume extrusion apparatus for preparation of large unilamellar vesicles, *Biochim. Biophys. Acta 1061*, 297−303.

37. Anderluh, G., Beseničar, M., Kladnik, A., Lakey, J. H., and Maček, P. (2005) Properties of nonfused liposomes immobilized on an L1 Biacore chip and their permeabilization by a eukaryotic pore-forming toxin, *Anal. Biochem. 344*, 43−52.

38. Hong, Q., Gutiérrez-Aguirre, I., Barlič, A., Malovrh, P., Kristan, K., Podlesek, Z., Maček, P., Turk, D., González-Mañas, J. M., Lakey, J. H., and Anderluh, G. (2002) Two-step membrane binding by equinatoxin II, a pore-forming toxin from the sea anemone, involves an exposed aromatic cluster and a flexible helix, *J. Biol. Chem. 277*, 41916−41924.

39. Malovrh, P., Barlič, A., Podlesek, Z., Maček, P., Menestrina, G., and Anderluh, G. (2000) Structure-function Studies of Tryptophan Mutants of Equinatoxin II, a Sea Anemone Pore-forming Protein, *Biochem. J. 346*, 223−232.

40. Cho, W., Bittova, L., and Stahelin, R. V. (2001) Membrane binding assays for peripheral proteins, *Anal. Biochem. 296*, 153−161.

41. Mozsolits, H., and Aguilar, M. I. (2002) Surface plasmon resonance spectroscopy: An emerging tool for the study of peptide-membrane interactions, *Biopolymers 66*, 3−18.

42. Beseničar, M., Maček, P., Lakey, J. H., and Anderluh, G. (2006) Surface plasmon resonance in protein-membrane interactions, *Chem. Phys. Lipids 141*, 169−178.

43. Cooper, M. A., Hansson, A., Lofas, S., and Williams, D. H. (2000) A vesicle capture sensor chip for kinetic analysis of interactions with membrane-bound receptors, *Anal. Biochem. 277*, 196−205.

44. Kahya, N., Scherfeld, D., Bacia, K., Poolman, B., and Schwille, P. (2003) Probing lipid mobility of raft-exhibiting model membranes by fluorescence correlation spectroscopy, *J. Biol. Chem. 278*, 28109−28115.

45. Veatch, S. L., and Keller, S. L. (2003) Separation of liquid phases in giant vesicles of ternary mixtures of phospholipids and cholesterol, *Biophys. J. 85*, 3074−3083.

46. Rich, R. L., and Myszka, D. G. (2005) Survey of the year 2003 commercial optical biosensor literature, *J. Mol. Recognit. 18*, 1−39.

47. Jacobs, T., Darji, A., Frahm, N., Rohde, M., Wehland, J., Chakraborty, T., and Weiss, S. (1998) Listeriolysin O: Cholesterol inhibits cytolysis but not binding to cellular membranes, *Mol. Microbiol. 28*, 1081−1089.

48. Rich, R. L., and Myszka, D. G. (2000) Advances in surface plasmon resonance biosensor analysis, *Curr. Opin. Biotechnol. 11*, 54−61.

49. Bonev, B. B., Gilbert, R. J., Andrew, P. W., Byron, O., and Watts, A. (2001) Structural analysis of the protein/lipid complexes associated with pore formation by the bacterial toxin pneumolysin, *J. Biol. Chem. 276*, 5714−5719.

50. Brogden, K. A. (2005) Antimicrobial peptides: Pore formers or metabolic inhibitors in bacteria? *Nat. Rev. Microbiol. 3*, 238−250.

51. Marsh, D. (1996) Lateral pressure in membranes, *Biochim. Biophys. Acta 1286*, 183−223.

52. Brockman, H. (1999) Lipid monolayers: Why use half a membrane to characterize protein-membrane interactions? *Curr. Opin. Struct. Biol. 9*, 438−443.

53. Ohno-Iwashita, Y., Iwamoto, M., Mitsui, K., Ando, S., and Iwashita, S. (1991) A cytolysin, θ-toxin, preferentially binds to membrane cholesterol surrounded by phospholipids with 18-carbon hydrocarbon chains in cholesterol-rich region, *J. Biochem. 110*, 369−375.

54. Heuck, A. P., Hotze, E. M., Tweten, R. K., and Johnson, A. E. (2000) Mechanism of membrane insertion of a multimeric β-barrel protein: Perfringolysin O creates a pore using ordered and coupled conformational changes, *Mol. Cell 6*, 1233−1242.

55. Rosenqvist, E., Michaelsen, T. E., and Vistnes, A. I. (1980) Effect of streptolysin O and digitonin on egg lecithin/cholesterol vesicles, *Biochim. Biophys. Acta 600*, 91−102.

56. Rottem, S., Cole, R. M., Habig, W. H., Barile, M. F., and Hardegree, M. C. (1982) Structural characteristics of tetanolysin and its binding to lipid vesicles, *J. Bacteriol. 152*, 888−892.

57. Pasenkiewicz-Gierula, M., Subczynski, W. K., and Kusumi, A. (1990) Rotational diffusion of a steroid molecule in phosphatidylcholine-cholesterol membranes: Fluid-phase microimmiscibility in unsaturated phosphatidylcholine-cholesterol membranes, *Biochemistry 29*, 4059−4069.

58. Subczynski, W. K., Antholine, W. E., Hyde, J. S., and Kusumi, A. (1990) Microimmiscibility and three-dimensional dynamic structures of phosphatidylcholine-cholesterol membranes: Translational diffusion of a copper complex in the membrane, *Biochemistry 29*, 7936−7945.

59. Lagane, B., Mazeres, S., Le Grimellec, C., Cezanne, L., and Lopez, A. (2002) Lateral distribution of cholesterol in membranes probed by means of a pyrene-labelled cholesterol: Effects of acyl chain unsaturation, *Biophys. Chem. 95*, 7−22.

60. Huang, J., and Feigenson, G. W. (1999) A microscopic interaction model of maximum solubility of cholesterol in lipid bilayers, *Biophys. J. 76*, 2142−2157.

61. Rebolj, K., Ulrih, N. P., Maček, P., and Sepčić, K. (2006) Steroid structural requirements for interaction of ostreolysin, a lipid-raft binding cytolysin, with lipid monolayers and bilayers, *Biochim. Biophys. Acta 1758*, 1662−1670.

62. Valeva, A., Hellmann, N., Walev, I., Strand, D., Plate, M., Boukhallouk, F., Brack, A., Hanada, K., Decker, H., and Bhakdi, S. (2006) Evidence that clustered phosphocholine head groups serve as sites for binding and assembly of an oligomeric protein pore, *J. Biol. Chem. 281*, 26014−26021.

63. Nollmann, M., Gilbert, R., Mitchell, T., Sferrazza, M., and Byron, O. (2004) The role of cholesterol in the activity of pneumolysin, a bacterial protein toxin, *Biophys. J. 86*, 3141−3151.

64. Zitzer, A., Westover, E. J., Covey, D. F., and Palmer, M. (2003) Differential interaction of the two cholesterol-dependent, membrane-damaging toxins, streptolysin O and *Vibrio cholerae* cytolysin, with enantiomeric cholesterol, *FEBS Lett. 553*, 229−231.

65. Cocklin, S., Jost, M., Robertson, N. M., Weeks, S. D., Weber, H. W., Young, E., Seal, S., Zhang, C., Mosser, E., Loll, P. J.,

Saunders, A. J., Rest, R. F., and Chaiken, I. M. (2006) Real-time monitoring of the membrane-binding and insertion properties of the cholesterol-dependent cytolysin anthrolysin O from *Bacillus anthracis*, *J. Mol. Recognit. 19*, 354−362.

66. Dubail, I., Autret, N., Beretti, J. L., Kayal, S., Berche, P., and Charbit, A. (2001) Functional assembly of two membrane-binding domains in listeriolysin O, the cytolysin of *Listeria monocytogenes*, *Microbiology 147*, 2679−2688.

67. Heuck, A. P., Tweten, R. K., and Johnson, A. E. (2003) Assembly and topography of the prepore complex in cholesterol-dependent cytolysins, *J. Biol. Chem. 278*, 31218−31225.

68. Palmer, M., Harris, R., Freytag, C., Kehoe, M., Tranum-Jensen, J., and Bhakdi, S. (1998) Assembly mechanism of the oligomeric streptolysin O pore: The early membrane lesion is lined by a free edge of the lipid membrane and is extended gradually during oligomerization, *EMBO J. 17*, 1598−1605.

69. Shaughnessy, L. M., Hoppe, A. D., Christensen, K. A., and Swanson, J. A. (2006) Membrane perforations inhibit lysosome fusion by altering pH and calcium in *Listeria monocytogenes* vacuoles, *Cell. Microbiol. 8*, 781−792.